Relaxation in bulk $R\mathrm{Ba_2Cu_3O_{7-\delta}}$ superconductors

M. Jirsa*
Institute of Physics ASCR, Na Slovance 2, CZ-182 21 Praha 8, Czech Republic

T. Nishizaki and N. Kobayashi
Institute for Material Research, Tohoku University, 2-1-1 Katahira, Aoba-ku, Sendai 980-77, Japan

M. Muralidhar and M. Murakami
Superconductivity Research Laboratory, ISTEC, 16-25 Shibaura 1-chome, Minato-ku, Tokyo 105-0023, Japan
(Received 16 July 2003; revised manuscript received 29 January 2004; published 30 July 2004)

The shape of the magnetic hysteresis curve, "MHL," in bulk strongly doped $R\mathrm{Ba_2Cu_3O_{7-\delta}}$ materials is analyzed and its correlation with relaxation characteristics is verified. It is shown that field and temperature dependencies of logarithmic relaxation rate, $Q = d\ln J / d\ln dB/dt$, can be obtained from $J(B)$ and $J(T)$ data (J is the supercurrent density associated with total magnetic moment). In the case of the MHL with two well-distinguished peaks, the two additive contributions to J are correlated with corresponding relaxation characteristics, which are given analytically. Plateau in $Q(T)$ dependence in such materials is shown to originate from scanning the specific shape of MHL at a fixed field. From $Q(J)$ plot pinning energy characteristics at low and intermediate fields are deduced.

DOI: 10.1103/PhysRevB.70.024525 PACS number(s): 74.25.Qt, 74.25.Sv, 74.72.−h

I. INTRODUCTION

In high-T_c materials, the induced magnetization, M, and the associated current density,[1,2] J, are strongly time-dependent.[3–5] Although the relaxation effects are much more pronounced than in conventional superconductors, they can be described by a classical theory extended for a nonlinear dependence of pinning barrier on supercurrent, $U(J)$. In this way, we can utilize relaxation characteristics for the study of material parameters and deduce properties of the particular pinning mechanisms or the associated pinning media.

In untwinned bulk $R\mathrm{Ba_2Cu_3O_{7-\delta}}$ (R=rare earth, RE-123) samples with *fishtail* or *second peak* effect, an enhancement of irreversible magnetic moment or associated supercurrent at intermediate and high fields is usually the most significant feature of magnetic hysteresis loop (MHL). This peak has been assigned to vortex pinning on a random distribution of point-like defects or nanometer scale clusters. Such disorder can arise from oxygen deficiency,[6–8] fluctuation of chemical composition due to solid solution of light rare earth elements with Ba (Refs. 9 and 10) or any other fluctuation of superconductor properties on nanometer scale.

The second peak develops a characteristic scaling that was extensively studied by Perkins *et al.* and put into the basis of their phenomenological model.[11] One of the central results of this model was the relationship between relaxation phenomena represented by the "dynamic" normalized relaxation rate, $Q = d\ln J / d\ln(dB/dt)$, and shape of MHL in terms of the logarithmic derivative $d\ln J / d\ln B$. Based on this model, a novel analytical formula was later derived,[12] successfully modeling shape of the second peak in a broad range of materials.[12–15]

The aim of this paper is to present new features of the relationship between relaxation phenomena and irreversible magnetization in bulk RE-123 samples with strong point-like pinning disorder. New consequences of this relationship shed light on typical shapes of experimentally observed field and temperature dependencies of the normalized relaxation rate.

II. EMPIRICAL MODEL

As our study deals with relaxation effects during magnetization processes, it is useful to recall some basic relationships between relaxation and pinning characteristics. Starting from the expression for activation energy, $U(J) = -kT[\ln|dJ/dt| - C_1]$, derived by Maley *et al.*[16] and using the proportionality $dJ/dt \propto dM/dt \propto dB/dt$ associated with magnetic field sweep (Been model), we arrive at $U(J) = -kT[\ln|dB/dt| - C_2]$, which is a modification of the Maley's formula for "dynamic" relaxation experiments.[4,17] By differentiating this formula with respect to $\ln J$, we get[17,18]

$$Q(B,T,J) = -kT\left(\frac{\partial U(B,T,J)}{\partial \ln J}\right)^{-1}. \tag{1}$$

Obviously, for the logarithmic pinning barrier, $U(J) = U_0(B,T)\ln(J_0/J)$, where U_0 and J_0 are material characteristics, Eq. (1) simplifies to

$$Q(B,T) = kT/U_0(B,T). \tag{2}$$

Note that the logarithmic pinning barrier has been found many times to be consistent with pinning on a point-like disorder,[11,12,19,20] associated with the second peak effect.

A. Second peak of MHL

The relationship between MHL shape and relaxation deduced by Perkins *et al.* from the experimentally observed *scaling* of the second peak with *electric field* reads[11]

$$Q(B) = \gamma_E[k_E - \chi_{ln}(B)], \tag{3}$$

where $\chi_{ln} = \partial \ln J / \partial \ln B$ is the logarithmic derivative of the MHL, and γ_E, k_E are parameters independent of field and only slightly temperature dependent. Typical values of these parameters in bulk RE-123 materials are $\gamma_E \approx 0.02-0.09$ (Refs. 11–14 and 21) and $k_E \simeq 1$.[11–13,15,22]

The model function describing shape of the MHL with second peak is[12]

$$J(B) = J_{max} B/B_{max} \exp[(1 - (B/B_{max})^n)/n], \tag{4}$$

where B_{max} and J_{max} are coordinates of the second peak maximum. Note that contrary to the original Perkins' model,[11,21,22] we consider $U_0 \propto B^{-n}$ and, therefore, n is here *positive*. Most of the experimentally determined values of n fall between 1 and 3.[3,11–13,15,20,22,23]

It is easy to show that $J(B)$ from Eq. (4) has just one inflexion point at

$$B_{inf} = B_{max} \sqrt[n]{n+1}. \tag{5}$$

Combining this result with logarithmic derivative of Eq. (4), $\chi_{ln}(B) = 1 - (B/B_{max})^n$ we get

$$n = -\chi_{ln}(B_{inf}). \tag{6}$$

This means that the constant n in Eq. (4) represents the highest logarithmic slope of the high-field shoulder of the secondary peak. Thus, the second peak is described by three parameters directly accessible from experimental data.

A simple calculation shows that

$$J(B_{inf})/J(B_{max}) = e^{-1} B_{inf}/B_{max} \cong 0.368 B_{inf}/B_{max}. \tag{7}$$

This relationship is independent of material parameters and implies that the shape of the second peak is a universal curve (as long as the simple MHL scaling with temperature utilized in the Perkins' model holds).

Equation (7) is useful for determination of n from experiment. Instead of the $J(B)$ curve derivative, the inflexion point can be estimated to a reasonable accuracy as the intersection with the line running from (0,0) with the slope $e^{-1} J_{max}/B_{max}$. Then, with the known B_{inf} it is easy to determine the tangent $n = -\partial \ln J / \partial \ln B|_{B_{inf}}$.

From Eqs. (4) and (3) we get

$$Q(B,T) = \gamma_E \left(\frac{B}{B_{max}(T)} \right)^n, \tag{8}$$

a monotonously increasing function of field. Equation (8) indicates that $\gamma_E = Q(B_{max})$. As γ_E is nearly temperature independent,[11,22] Q at the top of the second peak is practically independent of temperature, too.

Equation (8) is a consequence of the second peak scaling; it shows that Q does not change with temperature for any normalized field B/B_{max}.

From Eq. (2) we get the field and temperature dependent U_0 at high fields in the form

$$U_0(B,T) = \frac{kT}{\gamma_E} \left(\frac{B}{B_{max}(T)} \right)^{-n}. \tag{9}$$

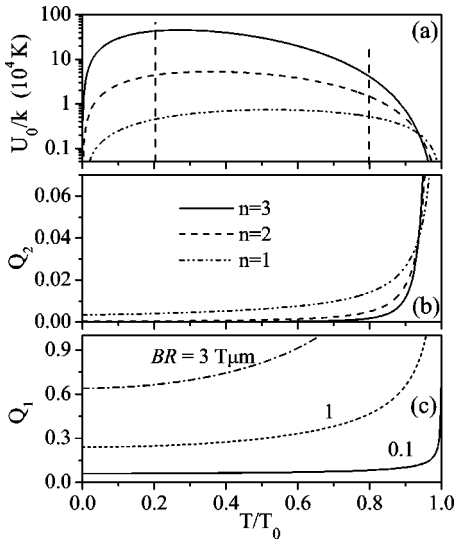

FIG. 1. Theoretical temperature dependencies of (a) U_0, (b) Q_2, and (c) Q_1 calculated according to Eqs. (9), (8), and (12), respectively. U_0 and Q_2 were determined for $n=1$, 2, and 3. $B_{max}(T) = 12(1-T/91)^{0.9}$ was deduced from experiment on melt-textured NEG-123 (see the text). $Q_1(T)$ is shown for three indicated values of *BR*. The vertical dash lines in (a) indicate the region within which comparison with experiment of Ref. 22 is possible.

Figures 1(a) and 1(b) display U_0/k and Q as a function of temperature according to Eqs. (9) and (8), respectively, for $n=1$, 2, and 3, and $B=1$ T. $B_{max}(T) = 12(1-T/91)^{0.9}$ was deduced from the experiment on NEG-123 sample "S1" (see below). Note that the characteristic temperature $T_0 = 91$ K, relating to the behavior of second peak, is close to but not necessarily identical with T_c. A similar $B_{max}(T)$ dependence has also been observed elsewhere.[20,24] Comparing Fig. 1(a) with the experiments on Tm-123 single crystals[22] [Fig. 7(b)], we see a qualitative resemblance of the curves with the present theoretical curve for $n=3$, which contradicts $n \approx 1$ estimated by the comprehensive analysis in Ref. 22. Equation (9) indicates that the main reason for the discrepancy might be a difference in $B_{max}(T)$ courses. Comparison of $B_{max}(T) = 12(1-T/91)^{0.9}$ with Fig. 5(b) in Ref. 22 shows that this is really the case. In the intermediate temperature range, $0.2-0.8\ T_c$, $U_0(T)$ is given by the interplay of the linear kT term and $[B_{max}(T)]^n$. Thus, the actual form of $U_0(T)$ strongly depends on the material characteristics, especially n and $B_{max}(T)$.

B. Central peak

Neither Eq. (4) nor Eq. (8) correctly describe the experimentally observed MHL shape at low fields. This is because the central peak in the low-field region exhibits another type of scaling[11,25–27] than the second peak and until now has been omitted in our analysis (as well as in most published treatments). In RE-123 single crystals without secondary phase precipitates, self-field effects, reflecting demagnetization, govern the low-field range of MHL.[11,28] In RE-123 melt-textured compounds, pinning by "large" normal particles significantly contributes.[25–27] The low-field contribution to the

total magnetic moment (current density) can be described by an exponentially decaying function,[12,15]

$$J(B) = J_{01} \exp(-B/B_L), \tag{10}$$

where B_L is a characteristic field and J_{01} is the magnitude of the central peak.

For pinning by "large" normal particles, $B_L = \Phi_0/(2\pi\xi R)$, where R is the mean radius of the secondary phase particles, Φ_0 is magnetic flux quantum, ξ is coherence length.[27] Thus, the exponential decay rate can be quite precisely estimated provided we know R from a structural analysis and checked by fit of experimental data.

Combining formally Eqs. (10) and (3), we get that the relaxation rate corresponding to pinning by "large" normal particles increases linearly with field as

$$Q(B) \approx \gamma_E(k_E + B/B_L). \tag{11}$$

We note that the use of Eq. (3) in the low field range is not exact as the scaling properties put into basis of the model are different.[11,29] Thus, at least γ_E and k_E require a generalization. This point will be discussed below. Bearing the same comment in mind, we can derive temperature dependence, $Q(T)$.

Temperature enters Eq. (11) through $B_L(T) \propto 1/\xi(T) \propto \sqrt{1-t^2}$, where $t = T/T_c$.[30] Thus $Q(T)$ acquires the explicit form

$$Q(T) \approx \gamma_E[k_E + \eta/\sqrt{(1-t^2)}], \tag{12}$$

where $\eta = 2\pi\xi(0)BR/\Phi_0$ is independent of temperature, $\xi(0)$ is the coherence length at $T=0$, and B is the constant magnetic field fixed during temperature sweep. With $\xi(0) \approx 1.5$ nm, η is approximately $4.6BR$ T^{-1} μm^{-1}.

As we have now two sets of J and Q, associated with the central and second peak contributions, for sake of clarity, we will further distinguish them by subscripts "1" and "2," respectively. Thus Q from Eq. (12) will be Q_1 and that from Eq. (8) will be Q_2, etc. The terms without subscript will further refer to the *total* quantities obtained as a sum of both contributions.

Evidently, the leading term in Eq. (12) close to T_c is $(1-t)^{-1/2}$, which is much slower than the term $(1-t)^{-n}$ governing $Q_2(T)$ [Eq. (8)] in the same temperature range. On the other hand, at low temperatures, except for very high magnetic fields, $B \gg B_{max}(0)$, $Q_1 > Q_2$. It can be seen from comparison of Figs. 1(b) and 1(c). The latter figure shows three $Q_1(T)$ curves for $k_E = 1$, $\gamma_E = 0.04$ and $BR = 0.1$, 1, and 3T μm. However, the effect of both pinning mechanisms to the total relaxation rate is not simply additive but modified by weighting factors as will be shown further.

C. Additive pinning

By summing the terms of the central and second peak, we get[15]

$$J(B) = J_{01} \exp(-B/B_L) + J_{max} B/B_{max} \exp[(1-(B/B_{max})^n)/n], \tag{13}$$

where J_{01}, J_{max} are magnitudes of the central and second peak, respectively. Usually, J_{01}, J_{max}, and B_{max} can be directly determined from experiment. As the first term in Eq. (13) decays rather fast, its contribution to J at around B_{inf} (the high-field inflexion point) is usually negligible. Therefore, n can be determined according to Eq. (6) as described above. Thus B_L remains the only adjustable parameter. With the $B_L$value obtained from MHL fit, the average value of R can be estimated as $R = \Phi_0/(2\pi\xi(T)B_L)$.

With help of Eq. (13) one can decompose the experimental $J(B)$ dependence into two terms, $J_1(B)$ and $J_2(B)$, and get better insight into the efficiency of the underlying pinning mechanisms in different fields.

Having two full MHLs measured with different field sweep rates, one can decompose each of them and calculate the "experimental" relaxation rates separately for the pinning mechanisms associated with the central and second peak, $Q_1(B) = \Delta \ln J_1(B)/\Delta \ln(dB/dt)$ and $Q_2(B) = \Delta \ln J_2(B)/\Delta \ln(dB/dt)$, respectively.

By differentiating Eq. (13) with respect to $\ln(dB/dt)$, we get

$$Q = Q_1 \frac{J_1}{J} + Q_2 \frac{J_2}{J}. \tag{14}$$

By substituting for Q_1 and Q_2, Eq. (14) reads

$$Q(B) = \frac{\gamma_E}{J(B)} \left[(1 + B/B_L) J_1(B) + \left(\frac{B}{B_{max}} \right)^n J_2(B) \right]. \tag{15}$$

Except for γ_E, which needs to be estimated by an independent relaxation experiment at B_{max}, all other parameters, B_{max}, B_L, and n are accessible from the MHL analysis. As γ_E is nearly temperature independent, only one relaxation experiment is needed for all temperatures. With known γ_E, $Q(B)$ can be in the whole experimental field range deduced from the shape of corresponding magnetic hysteresis loop.

Due to the central peak contribution, two additional inflexion points appear on $J(B)$ dependence, one lying on the right shoulder of central peak and the other on the low-field side of second peak. These two inflexion points correlate in turn with the shallow maximum and minimum on $Q(B)$.

At all extremes of the $J(B)$ curve (the maxima of central and second peak and the intermediate minimum), $\chi_{ln} = 0$ and, therefore, $Q = \gamma_E$. Thus, Q is up to B_{max} rather a weak function of B, slightly fluctuating around γ_E value. Here we again stress that γ_E and k_E are not at low fields well defined parameters in terms of the Perkins' model.

The central peak contribution is also reflected in temperature dependence of Q. This dependence is usually measured by ramping temperature and holding field, B, fixed. For clarity, we will denote this field as B_f. On the other hand, irreversibility field, together with the whole MHL, scales with temperature. Thus, during temperature ramping the relation between B_f and characteristic features of the MHL changes and one in fact scans the MHL or $J(B)$ curve.

Let at some relatively low temperature T_1, B_f lie well below $B_{max}(T_1)$. From the above discussion it follows that $Q(B_f, T_1) \approx \gamma_E$. With increasing temperature, $B_{max}(T)$ shifts toward B_f. During this shift $Q(B_f, T)$ slightly fluctuates around γ_E value up to the moment when B_f at some temperature T_2 exceeds $B_{max}(T_2)$. Above this temperature a rapid rise

of $Q(B_f, T)$ occurs, in correspondence with experimental observations. For bulk RE-123 superconductors, this is a natural explanation of the plateau on $Q(T)$ commonly observed in low/intermediate temperatures. Both the present explanation and experiment[31] show a broad plateau for low magnetic fields [where the difference between B_f and $B_{max}(T_1)$ is large], a narrower one as the distance between B_f and $B_{max}(T_1)$ decreases, and finally a reduction of the plateau into a point when $B_f \geq B_{max}(T_1)$. A similar plateau on $Q(T)$ observed in thin films,[32] where $J(B)$ is a monotonously decreasing function, has most probably another ground as $J(B)$ dependence in thin films is governed by a completely different pinning (and relaxation) mechanism.

III. EXPERIMENT

Most of the above-described results will be demonstrated on a melt-textured $(Nd_{0.33}Eu_{0.33}Gd_{0.33})Ba_2Cu_3O_y$ (NEG-123) sample with addition of 30 mol % Gd_2BaCuO_5 particles. This sample, denoted "S1," exhibited magnetic hysteresis loop with two well-distinguished peaks separated by a deep minimum, typical for many untwined bulk RE-123 materials. It was produced by means of oxygen-controlled-melt-growth process described in detail in Ref. 15. Structural analysis reported there (sample LLM) revealed a uniform dispersion of the secondary phase particles of 0.1 to a few μm in diameter. Point-like disorder was mainly due to RE/Ba compositional fluctuation.[9,10] Oxygen deficiency was minimal because of optimum oxygenation ($T_c \approx 93$ K). Twin boundaries were absent. Sample "S2" was a melt-textured $(Nd_{0.33}Eu_{0.38}Gd_{0.28})Ba_2Cu_3O_y$ with 5 mol % of $(Nd_{0.33}Eu_{0.33}Gd_{0.33})_2BaCuO_5$ and was produced by the same technology as S1. The particular Nd-Eu-Gd ratio resulted in twinning. The twin structure consisted of regular twins and a fine nano-scale lamellar substructure aligned with the regular twins.[33] This special type of pinning medium caused an anomalous enhancement of pinning at very high fields, a shift of the second peak to higher fields, and a partial filling of the minimum between central and second peak so that the dip transformed into a plateau.

Magnetic measurements were performed by means of a vibrating sample magnetometer (VSM) in the field range up to 14 T, mostly with field sweep rates 0.7, 0.4, and 0.2 or 0.1 T/min. The *experimental* $Q(B)$ curves were calculated as a logarithmic difference of two full hysteresis curves measured with field sweep rates 0.7 and 0.2 or 0.1 T/min. The *model* $Q(B)$ was obtained from Eq. (3) using logarithmic derivatives $\chi_{ln}(B)$ of MHLs measured with the intermediate field sweep rate (0.4 or 0.3 T/min). γ_E was determined according to definition from the shift of the secondary peak with field sweep rate. Supercurrent density J was calculated from the measured irreversible magnetic moment using the extended Bean model,[1,2] $J = \Delta M / [a^2 c(b - a/3)/2]$, where a, b, c are dimensions of the rectangular sample and ΔM is the height of MHL.

IV. EXPERIMENTAL RESULTS AND DISCUSSION

The correlation of the characteristic points of $J(B)$ and $Q(B)$ dependencies is demonstrated in Fig. 2. Figure 2(a) shows the $J(B)$ curve of sample S1 recorded at 70 K with field sweep rate 0.4 T/min. Characteristic points of the curve are marked by vertical lines; the extremes by dot-and-dash ones, the inflexion points by dotted ones. These lines coincide with the corresponding features of $Q(B)$ and $-\chi_{ln}(B)$ dependencies shown in Fig. 2(b). At $J(B)$ extremes, $Q(B) = \gamma_E$ [as $\chi_{ln}(B) = 0$], at the middle inflexion point of $J(B)$, both $-\chi_{ln}(B)$ and $Q(B)$ reach their minimum values. Thus, $Q(B)$ starts increasing *significantly below* B_{max}. At and around B_{max}, $Q(B)$ has always a positive slope. The lowest-lying inflexion point can be approximately associated with a shallow maximum of $Q(B)$ at low fields. No significant feature of $Q(B)$ corresponds to the high-field inflexion point, $J(B_{inf})$.

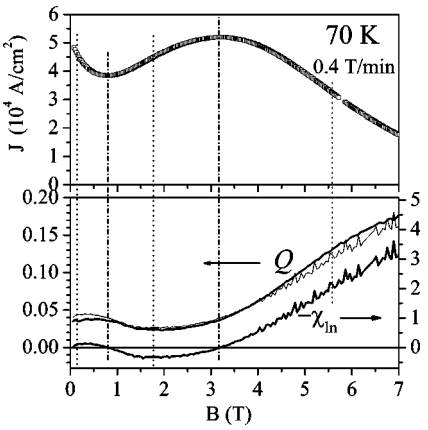

FIG. 2. Correlation of the experimental $J(B)$ dependence (a) with $Q(B)$ and $-\chi_{ln}(B)$ (b) of sample S1 for 70 K and field sweep rate 0.4 T/min. $Q(B)$ was determined as $\Delta \ln J / \Delta \ln(dB/dt)$ from the $J(B)$ curves measured with sweep rates of 0.7 and 0.1 T/min (thick solid curve) and from Eq. (3) using $J(B)$ measured with 0.4 T/min (thin noisy curve). The vertical dot-dash and dotted lines indicate correlation of extremes and inflexion points of $J(B)$ with zero and extreme points of $Q(B)$, respectively.

The two ways of $Q(B)$ calculation are indicated by different line styles. That calculated from two complete MHL curves measured with slightly different field sweep rates is the thicker one. That obtained by means of Eq. (3) with $-\chi_{ln}(B)$ from one complete MHL and γ_E determined separately is thinner and more noisy. γ_E was estimated as $Q(B_{max}) = [\Delta \ln J / \Delta \ln(dB/dt)]_{B=B_{max}}$ calculated from short sections of two MHLs measured with different field sweep rates around B_{max}. Both approaches are almost equivalent. Obviously, all features of $-\chi_{ln}(B)$ are reflected by $Q(B)$.

Figures 3(a) and 3(c), together with Fig. 2, document that although the $J(B)$ dependence does not scale in a wide temperature range, the correlation between $J(B)$ and $Q(B)$ dependencies persists over the whole temperature region, irrespective of the field range reduction and the relative second peak height decrease. The faster decrease of the second peak with increasing temperature with respect to the central peak is consistent with higher pinning energy of the relatively large secondary phase particles with respect to nanometer-size point-like defects. It is natural that with increasing thermal activation the pinning efficiency of small point-like de-

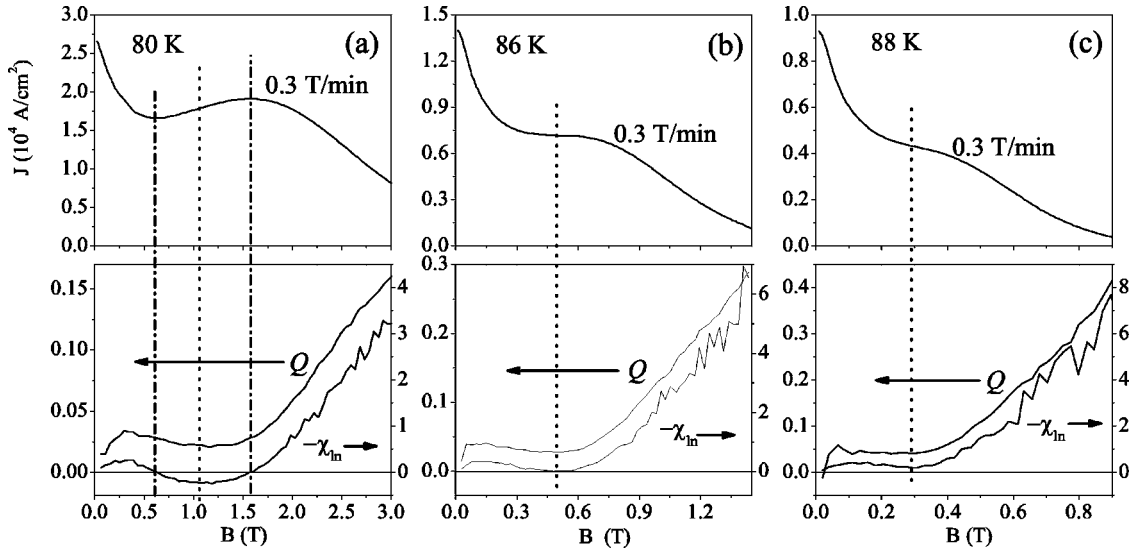

FIG. 3. Correlation of $J(B)$ dependencies (upper figures) with $Q(B)$ and $-\chi_{\ln}(B)$ (lower figures) of the sample S1 for 80 K (a), 86 K (b), and 88 K (c). The measurements were made with $dB/dt=0.3$ T/min. $Q(B)$ were determined as $\Delta \ln J/\Delta \ln(dB/dt)$ from the curves measured with field sweep rates of 0.7 and 0.1 T/min. The vertical dot-dash and dotted lines indicate correlation between extremes and inflexion points of the $J(B)$ dependence with zero and extreme points of $Q(B)$, respectively.

fects drops much faster than that of large particles. Moreover, as irreversibility field drops with increasing temperature, the field range of the pinning dominated by point-like defects gradually reduces in favor of large particles. Thus, with increasing temperature the secondary peak rapidly diminishes, changes into a shoulder on the MHL, and finally vanishes. Consistently, the $-\chi_{\ln}(B)$ and $Q(B)$ minima transform into broad plateaus [Fig. 3(b)] and, finally, close to T_c, the curves become monotonously increasing functions [see, e.g., 3(a) in Ref. 34]. On the other hand, in RE-123 single crystals only a limited number of "large" particles is present and the central peak is controlled by relatively weak self-field effects.[11,28] There, the central peak decreases with increasing temperature faster than the secondary peak.[12]

In Fig. 4 we show that the correlation between $J(B)$ and $Q(B)$ exists also for the decomposed components.[35] The dotted and dot-dash curves in Fig. 4(a) describe the central and second peak components, respectively. The solid curve representing the theoretical total $J(B)$ dependence Eq. (13) can hardly be distinguished from the experimental data (symbols). The $Q_i(B)$ dependencies corresponding to the two $J_i(B)$ components, $i=1,2$, are displayed in Fig. 4(b). The curves were calculated from Eqs. (8) and (11), using only one complete MHL, measured with the intermediate field sweep rate 0.4 T/min. γ_E(=0.0394) was determined from a short segment of another experimental MHL measured with 0.7 T/min around $B_{\max}=3.21$ T. $J_{01}=51350$ A/cm^2 and $B_{\max}$ were determined directly from the experimental MHL, $J_{\max}=51213$ A/cm^2, $B_L=0.75$ T, and $n=2.09$ resulted from fit of the complete MHL by Eq. (13). Note that with this value of B_L and $\xi(0)=1.5$ nm, we get $R=1.93$ μm, which is in a very good agreement with the structural analysis of this sample.[15] Figure 4(c) shows the weighted components $Q_1(B)J_1(B)/J(B)$ and $Q_2(B)J_2(B)/J(B)$ and their sum. The total $Q(B)$ obtained in this way, represented by the thick solid curve, agrees with the curve calculated directly from difference of two full hysteresis curves so well that the curves are nearly indistinguishable [Fig. 4(c)]. The two vertical dashed lines in Fig. 4(c) delimit the area outside which only one of the weighted components $Q_1(B)J_1(B)/J(B)$ and $Q_2(B)J_2(B)/J(B)$ has a considerable magnitude: at low fields, $Q(B)$ is exclusively governed by the low-field pinning mechanism, $Q\approx Q_1$, at high fields only the high-field pinning

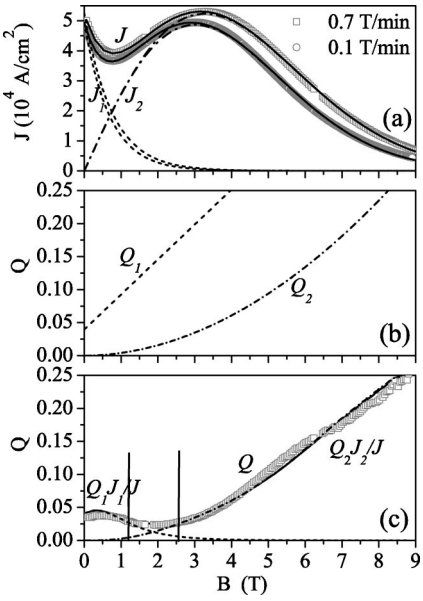

FIG. 4. (a) Decomposition of the $J(B)$ dependencies of the sample S1 measured at 70 K with field sweep rates 0.7 and 0.1 T/min into additive components, $J_1(B)$ (dotted curves) and $J_2(B)$ (dot-dash curves); (b) individual relaxation rates $Q_1(B)$ and $Q_2(B)$ calculated as $\Delta \ln J_i/\Delta \ln(dB/dt)$, $i=1,2$; (c) weighted individual relaxation rates, Q_1J_1/J and Q_2J_2/J, together with their sum (solid curve) and the "experimental" $Q(B)$ dependence obtained as $\Delta \ln J/\Delta \ln(dB/dt)$ (symbols).

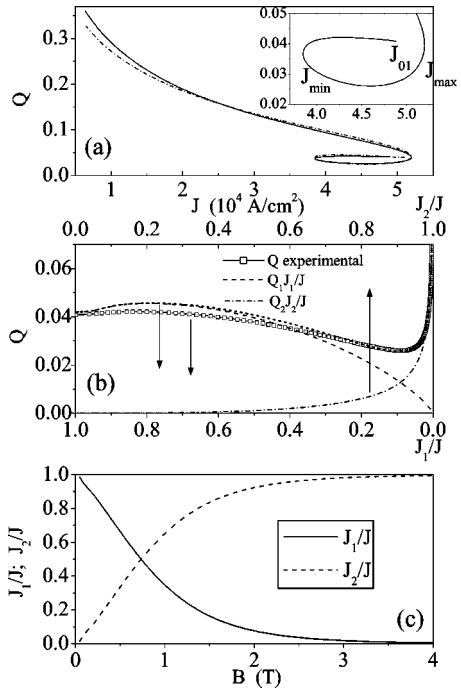

FIG. 5. Correlation of $J(B)$ dependence (upper figure) with $Q(B)$ and $\chi_{\ln}(B)$ (lower figure) of a twinned sample S2 at 77 K. The measurements were made with field sweep rates 0.7, 0.3, and 0.1 T/min. The vertical dotted and dot-dash lines indicate correlation between inflexion point and extremes of $J(B)$ with extreme and zero point of $Q(B)$, respectively.

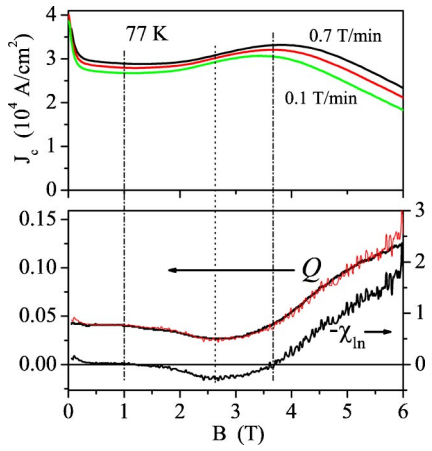

FIG. 6. Correlation of $J(B)$ dependence (upper figure) with $Q(B)$ and $-\chi_{\ln}(B)$ (lower figure) of a twinned sample S2 at 77 K. The measurements were made with field sweep rates 0.7, 0.3, and 0.1 T/min. The vertical dotted and dot-dash lines indicate correlation between inflexion point and extremes of $J(B)$ with extreme and zero point of $Q(B)$, respectively.

mechanism is important, $Q \approx Q_2$. Between the two lines, around the minimum of $Q(B)$, both contributions are of the same importance and have to be taken into account.

Another view of the above arguments we can find on the plot of Q as a function of J. Such a plot [Fig. 5(a)] exhibits three clearly distinguished parts: a nearly constant one between J_{01} and $J_{\min}$ (see the inset), a slightly (approximately parabolically) J-dependent one between $J_{\min}$ and $J_{\max}$, and finally, one increasing approximately logarithmically with decreasing J between $J_{\max}$ and low values of J (this part corresponds to the high-field slope of the MHL). The solid line represents experimental data (Q calculated from a difference of two curves measured with different sweep rates), the dashed line is the plot of Q from Eq. (15) with J calculated by means of Eq. (13) versus experimental J data. The experimental and theoretical curves are in a very good agreement in the whole field range. The first part, related to the central peak, is emphasized in the representation shown in Fig. 5(b) that presents Q and $Q_1 J_1/J$ as a function of J_1/J. Q can be in this range quite well approximated by the weighted dependence $Q_1 J_1/J$, up to about 0.3 J_1/J, which in turn corresponds to $B \approx 1$ T [see Fig. 5(c)]. The linear increase of $Q_1(B)$ according to Eq. (11) is in this field range satisfactorily compensated by the approximately linear drop of J_1/J with increasing B [Fig. 5(c)].

The third part of the curve in Fig. 5(a), corresponding to the fields $B \geqslant B_{\max}$, represents a modified logarithmic dependence. This seems to be inconsistent with Eq. (2) that claims Q to be independent of J. The explanation stacks in the fact that J is not an independent variable in magnetic measurements. Similar to Q, J depends on B. Substituting in Eq. (2) for B an inverse function to $J(B)$, $B = \mathrm{Inv}(J(B))$, where $J(B)$ is given by Eq. (13), one gets the dependence displayed in Fig. 5(a) (dashed line). Figure 5(b) shows that Q is in this field range very well approximated by $Q_2 J_2/J$ (the dot-dash line). The experimental data of $Q(J)$ merge with the approximate curve, $Q_2 J_2/J$, at about $Q = \gamma_E$, i.e., at $B_{\max}$.

$Q(B)$ is at low fields nearly constant. This implies that $U(J) \propto \ln J$ [Eq. (1)]. Thus, we can express $U(J)$ in the same way as for the second peak, $U(J) = U_0(B,T)\ln(J_0/J)$. Then, for the same reason as mentioned above for $Q(J)$ dependence at high fields, it follows from Eq. (2) that U_0 is independent of B. Consequently, any potential $U(B)$ dependence at low fields would originate solely from a difference in field dependencies of J_0 and J.

In the intermediate region, between $J_{\min}$ and $J_{\max}$, the $Q(J)$ dependence in Fig. 5(a) is evidently affected by both pinning mechanisms. Sum of both contributions, $Q_1 J_1/J + Q_2 J_2/J$, gives an excellent approximation of $Q(J)$ in this field range. Because the activation energy proved to be a logarithmic function of J both in the low- and high-field region, we can deduce that this is also true in the intermediate fields. Thus, Eq. (2) should hold there, too. However, the field dependence of U_0 is a rather complicated function.

The fact that the correlation between $J(B)$ and $Q(B)$ curves was verified at low fields, too, means that γ_E and k_E do not need a substantial modification due to a different scaling of the central peak.

Although the Perkins' model has been usually tested on samples with a distinguished second peak,[34,36] it should apply for any scaling characteristic feature of MHL.[11,21] This fact is demonstrated in Fig. 6 which presents data measured on *twinned* sample "S2." Here, the dip between the central and second peak was filled due to twin planes activity.[37] The shallow plateau-like minimum between the two peaks was observed only when magnetic field was applied along c axis

(along twin planes). The plateau transformed into a regular deep dip when the sample was declined by about 20° out of *c* axis. $Q(B)$ was nearly constant over the plateau, in correspondence with $\chi_{ln} \approx 0$ and the Q value was close to that obtained at B_{max}. Minimum relaxation rate was observed in the vicinity of the inflexion point on the low-field side of the second peak, in correspondence with the above model.

Similar evidence for a twinned sample was published in Ref. 38, where in *twinned* Y-123 single crystal magnetized along *c* axis a wavy broad maximum was observed instead of a second peak. The $Q(B)$ curves reflected all features of this anomalous MHL. After declining the sample by 20° from *c* axis, the wavy plateau of the MHL transformed into a regular second peak and the $Q(B)$ dependence also changed shape correspondingly. Although the other samples exhibited qualitatively the same correlation between $Q(B)$ and $J(B)$, the quantitative comparison is worse, probably due to the fact that the magnetic and relaxation data were recorded discretely by a superconducting quantum interference device (SQUID). Also the study by Werner *et al.*[39] on Y-123 single crystals by SQUID, VSM, and torque magnetometry gives typical $Q(B)$ dependencies (see the data for 50 K in Figs. 3 and 7 and for 60 K in Figs. 5, 8). The correlation of $Q(B)$ and $J(B)$ and its consistent change after irradiation by Pb ions was observed in Ref. 13 on a Dy-123 single crystal (see Fig. 5 therein).

The above phenomenological model is based on the experimentally observed scaling of a characteristic feature of MHL with electric field and temperature. Within this model, the answer to the basic question of what is the microphysical reason for $J(B)$ increase below B_{max}, can be only speculative. We therefore add only a few comments concerning the matter. Formally, the scale factor $J_0 \propto B^{k_E}$ is responsible for the increase of $J(B)$. We point out that $k_E \approx 1$ has been observed in a wide range of bulk RE-123 materials, which makes this dependence remarkably universal.

The correlation of the $Q(B)$ dependence with the shape of MHL excludes all solely static explanations of the second peak effect from consideration and points to a significant role of relaxation. On the other hand, the orthodox "dynamic" explanations, like that due to enhanced relaxation in the range of the dip between the central and second peak, also fail; we showed that the effective total relaxation rate is in all this field range rather low and practically temperature independent. We stress that the second peak (and the whole MHL) results from a delicate balance between relaxation and magnetic induction, in which the pinning strength plays an important role. Thus, for formation of MHL both static and dynamic effects are equally important.

A wide field for discussion is elastic properties of vortex matter. It was suggested that $J(B)$ rise can be due to shear modulus softening. However, maximum of $C_{66}(B) \propto b(1-b)^2(1-0.58b+0.29b^2)$ (with $b=B/B_{c2}$) lies at about $0.3\,B_{c2}$. Therefore, the explanation can be correct only in clean single crystals or conventional superconductors, where the peak appears close below B_{c2}. In high-T_c superconductors instead of B_{c2} we should take B_{irr} or B_m, the melting field, as a scale field. In strongly doped RE-123 materials $B_m \approx B_{irr}$ and thus, the maximum of C_{66} lies in the range of B_{max}. Consequently, in the relevant field range, C_{66} develops with field in a similar manner as the second peak in $J(B)$. Evidently, the classical theory has no satisfactory answer to this phenomenon and a new approach is needed.

The differentiation between point-like defects or their small clusters and "large" particles, each of them being responsible for another peak in MHL, is also not very reliable. The 20–50 nm large Zr-rich particles formed in a (Nd,Eu,Gd)-123 bulk after a long-term ZrO_2 ball milling of the secondary phase Gd-211 enormously enhanced J but especially at low field.[40] The work gave no evidence of a pinning mechanism crossover from "large" particle pinning (central peak) to the point-like disorder pinning (second peak). Even more striking was a similar behavior of the very homogeneous pinning structure of only 3–6 nm in size produced by fast neutron irradiation.[41–43] Again, a strong effect on J was observed, especially in the low field range. This might indicate that the pinning mechanism associated with the second peak involves some still unknown or not yet recognized feature.

V. SUMMARY AND CONCLUSIONS

Analyzing the relationship between logarithmic relaxation rate, Q, and logarithmic susceptibility, χ_{ln}, in which the scaling of magnetization in bulk strongly pinned RE-123 materials plays a principal role,[11,21] we found new features that shed light on several aspects of the model. (i) $J(B)$ around and above the second peak is in the case of logarithmic pinning potential a universal curve characterized by only one parameter, n, determining the logarithmic slope of $J(B)$ at its high-field inflexion point. (ii) $Q(B)$ is in the whole experimental field range determined by γ_E, the normalized relaxation rate at B_{max} (or at another MHL extreme), and by the logarithmic derivative of $J(B)$ [or $M(B)$]. (iii) Although the parameters γ_E and $k_E(\approx 1)$ were originally defined only for high fields, it occurs that the correlation between experimental and model $J(B)$ and $Q(B)$ data in RE-123 samples with a strong point-like pinning disorder persists also in the range of the central peak, which indicates that the parameters are nearly constant up to lowest fields. (iv) Equation (13) allows for separation of the two terms and an individual study of relaxation in the separate pinning regimes. The corresponding logarithmic relaxation rates enter the total relaxation rate, $Q(B)$ in the weighted form according to Eq. (15). (v) As $Q(B)=\gamma_E$ at any extreme of $J(B)$, the $Q(B)$ dependence is rather flat below B_{max}, slightly fluctuating around the value γ_E. Above B_{max}, $J(B)$ is usually only negligibly affected by central peak and thus $Q(B)$ increases as B^n (n reaching values between 1 and 3), being solely governed by the second peak pinning mechanism. (vi) From the experimental $Q(J)$ data of sample S1 at 70 K we deduced that the ansatz $U=U_0 \ln(J_0/J)$ and, therefore, also Eq. (2) can be used in all fields. Then, $U_0 \propto B^{-n}$ at high fields but $U_0(B)=$const at around central peak. In the intermediate fields, U_0 is a complicated function of B because both pinning mechanisms significantly participate. (vii) Fixing of magnetic field during temperature ramping between temperatures T_1 and T_2

$(T_1 < T_2)$ at a value B_f results in an effective scanning of the MHL between $B_f/B_{max}(T_1)$ and $B_f/B_{max}(T_2)$. If T_2 is set so that $B_{max}(T_2)=B_f \ll B_{max}(T_1)$, one gets a flat, slightly wavy $Q(T)$ dependence between T_1 and T_2, similar to the $Q(B)$ course at low fields, $B \leqslant B_{max}$. Above T_2, $Q(T)$ steeply increases up to T_c. This is a natural explanation of the plateau in $Q(T)$ dependence in bulk RE-123 samples with strong pinning. The plateau disappears when $B_f \geqslant B_{max}(T_1)$. (viii) The experimental evidence shows that the correlation between $J(B)$ and $Q(B)$ is valid in any RE-123 material exhibiting scaling of a significant feature of MHL with electric field, e.g., in twinned or irradiated samples. In such cases, the exact analytical $J(B)$ dependence is not known and the correlation can be verified only numerically. (ix) The equivalence between the dynamic relaxation rate and the conventional one,[44,45] allows for a substantial reduction of experimental time in the above type of analysis by measuring one full hysteresis loop and a short part of another one, around B_{max}, instead of a time-consuming measurement of conventional relaxation at a number of different fields.

ACKNOWLEDGMENTS

This work was accomplished under the support of grant GAAS of CR, No. K 1010104. M.J. acknowledges the financial support of JSPS in 2001 and 2002 that enabled him to stay at the Institute for Material Research, Tohoku University, Sendai, where most of the present experiments were made. Most of the samples were prepared in SRL/ISTEC, Morioka.

*Electronic address: jirsa@fzu.cz

[1] C. P. Bean, Rev. Mod. Phys. **36**, 2489 (1964).
[2] D. X. Chen and R. B. Goldfarb, J. Appl. Phys. **66**, 2489 (1989).
[3] Y. Yeshurun and A. P. Malozemoff, Phys. Rev. Lett. **60**, 2202 (1988).
[4] L. Pust, J. Kadlecová, M. Jirsa, and S. Durcok, J. Low Temp. Phys. **78**, 179 (1990).
[5] R. Griessen, Physica C **172**, 441 (1991).
[6] A. A. Zhukov, H. Küpfer, G. Perkins, L. F. Cohen, A. D. Caplin, S. A. Klestov, H. Claus, V. I. Voronkova, T. Wolf, and H. Wühl, Phys. Rev. B **51**, 12 704 (1995).
[7] A. Erb, J.-Y. Genoud, F. Marty, F. Däumling, E. Walker, and R. Flückiger, J. Low Temp. Phys. **105**, 1023 (1996).
[8] H. Küpfer, Th. Wolf, C. Lessing, A. A. Zhukov, X. Lançon, R. Meier-Hirmer, W. Schauer, and H. Wühl, Phys. Rev. B **58**, 2886 (1998).
[9] T. Egi, K. Kuroda, H. Unoki, and N. Koshizuka, Appl. Phys. Lett. **67**, 2406 (1995).
[10] N. Chikumoto, J. Yoshioka, and M. Murakami, Physica C **291**, 79 (1997).
[11] G. K. Perkins, L. F. Cohen, A. A. Zhukov, and A. D. Caplin, Phys. Rev. B **51**, 8513 (1995).
[12] M. Jirsa, L. Pust, D. Dlouhy, and M. R. Koblischka, Phys. Rev. B **55**, 3276 (1997).
[13] M. Jirsa, M. R. Koblischka, and A. J. J. van Dalen, Supercond. Sci. Technol. **10**, 484 (1997).
[14] M. Jirsa and L. Pust, Physica C **291**, 17 (1997).
[15] M. Jirsa, M. Muralidhar, M. Murakami, K. Noto, T. Nishizaki, and N. Kobayashi, Supercond. Sci. Technol. **14**, 50 (2001).
[16] M. P. Maley, J. O. Willis, H. Lessure, and M. E. McHenry, Phys. Rev. B **42**, 2639 (1990).
[17] M. Jirsa, L. Půst, H. G. Schnack, and R. Griessen, Physica C **207**, 85 (1993).
[18] A. J. J. van Dalen, M. R. Koblischka, and R. Griessen, Physica C **259**, 157 (1996).
[19] E. Zeldov, N. M. Amer, E. Koren, A. Gupta, M. W. McElfresh, and R. J. Gambino, Appl. Phys. Lett. **56**, 680 (1990).
[20] M. E. McHenry, S. Simizu, H. Lessure, M. P. Maley, J. Y. Coulter, I. Tanaka, and H. Kojima, Phys. Rev. B **44**, 7614 (1991).
[21] G. K. Perkins and A. D. Caplin, Phys. Rev. B **54**, 12 551 (1996).
[22] G. K. Perkins, L. F. Cohen, A. A. Zhukov, and A. D. Caplin, Phys. Rev. B **55**, 8110 (1997).
[23] M. Jirsa, M. R. Koblischka, M. Muralidhar, T. Higuchi, and M. Murakami, Physica C **338**, 235 (2000).
[24] T. Mochida, N. Chikumoto, and M. Murakami, Phys. Rev. B **62**, 1350 (2000).
[25] M. Murakami, H. Fujimoto, S. Gotoh, K. Yamaguchi, N. Koshizuka, and S. Tanaka, Physica C **185-189**, 321 (1991).
[26] M. Muralidhar, M. R. Koblischka, P. Diko, and M. Murakami, Appl. Phys. Lett. **76**, 91 (2000).
[27] V. Zablotskii, M. Jirsa, and P. Petrenko, Phys. Rev. B **65**, 224508 (2002).
[28] M. Daumling, E. Walker, and R. Flukiger, Phys. Rev. B **50**, 13 024 (1994).
[29] Y. Yeshurun, A. P. Malozemoff, and A. Shaulov, Rev. Mod. Phys. **68**, 911 (1996).
[30] M. Tinkham, in *Introduction to Superconductivity*, 2nd ed. (McGraw-Hill, New York, 1996).
[31] A. J. J. van Dalen, M. R. Koblischka, H. Kojo, K. Sawada, T. Higuchi, and M. Murakami, Supercond. Sci. Technol. **9**, 659 (1996).
[32] H. H. Wen, H. H. Schnack, R. Griessen, B. Dam, and J. Rector, Physica C **241**, 353 (1995).
[33] M. Muralidhar, M. Jirsa, H. Wu, N. Sakai, and M. Murakami, Supercond. Sci. Technol. **15**, 1357 (2002).
[34] T. Mochida, N. Chikumoto, and M. Murakami, Phys. Rev. B **64**, 064518 (2001).
[35] M. Jirsa, M. R. Koblischka, T. Higuchi, and M. Murakami, Phys. Rev. B **58**, R14 771 (1998).
[36] H. Küpfer, S. N. Gordeev, W. Jahn, R. Kresse, R. Meier-Hirmer, T. Wolf, A. A. Zhukov, K. Salama, and D. Lee, Phys. Rev. B **50**, 7016 (1994).
[37] Presence of twin planes usually results in a depression of the second peak. This effect was attributed to redistribution of supercurrents due to additional in-plane anisotropy (Ref. 35). Sometimes, instead of the peak depression, a filling of the preceding dip (between the central and second peak) is observed. It is not yet clear what is the reason for the different behavior.
[38] M. Jirsa, M. R. Koblischka, M. Murakami, G. Perkins, and A. D.

Caplin, Physica B **284-288**, 851 (2000).
[39] M. Werner, G. Branstätter, F. M. Sauerzopf, H. W. Weber, A. Hoekstra, R. Surdeanu, R. J. Wijngaarden, R. Griessen, Y. Abulafia, Y. Yeshurun, K. Winzer, and B. W. Veal, Physica C **303**, 191 (1998).
[40] M. Muralidhar, N. Sakai, M. Jirsa, N. Koshizuka, and M. Murakami, Appl. Phys. Lett. **83**, 5005 (2003).
[41] F. M. Sauerzopf, H. P. Wiesinger, H. W. Weber, and G. W. Crabtree, Phys. Rev. B **51**, 6002 (1995).
[42] F. M. Sauerzopf, Phys. Rev. B **57**, 10 959 (1998).
[43] M. Werner, F. M. Sauerzopf, H. W. Weber, and A. Wisniewski, Phys. Rev. B **61**, 14 795 (2000).
[44] M. Jirsa and L. Pust, IEEE Trans. Magn. **MAG-30**, 846 (1994).
[45] A. J. J. van Dalen, M. R. Koblischka, and R. Griessen, Physica C **259**, 157 (1996).